



## OPEN

# *In vitro* molecular evolution yields an NEIBM with a potential novel IgG binding property

SUBJECT AREAS:

PHAGE BIOLOGY

MICROBIOLOGY TECHNIQUES

Received  
28 February 2014Accepted  
14 October 2014Published  
4 November 2014Correspondence and  
requests for materials  
should be addressed to  
W.P. (pwpanwei@  
126.com)\* These authors  
contributed equally to  
this work.Peipei Qi<sup>1\*</sup>, Ying-Ying Ding<sup>1\*</sup>, Ting He<sup>1</sup>, Tong Yang<sup>2</sup>, Qiuli Chen<sup>1</sup>, Jiaojiao Feng<sup>1</sup>, Jinhong Wang<sup>1</sup>,  
Mingmei Cao<sup>1</sup>, Xiangyu Li<sup>1</sup>, Heng Peng<sup>1</sup>, Huaimin Zhu<sup>1</sup>, Jie Cao<sup>1</sup> & Wei Pan<sup>1</sup><sup>1</sup>Department of Medical Microbiology and Parasitology, School of Basic Medicine, Second Military Medical University, Shanghai 200433, China, <sup>2</sup>Fudan-Zhangjiang Bio-pharmaceutical Co., Ltd., Shanghai 201203, China.

*Staphylococcus aureus* protein A (SpA) and protein G of groups C and G streptococci (SpG) are two well-defined bacterial immunoglobulin (Ig)-binding proteins (IBPs) with high affinity for specific sites on IgG from mammalian hosts. Both SpA and SpG contain several highly-homologous IgG-binding domains, each of which possesses similar binding characteristic of the whole corresponding proteins. Whether specific combinations of these domains could generate a molecule with novel IgG-binding properties remained unknown. We constructed a combinatorial phage library displaying randomly-rearranged A, B, C, D and E domains of SpA as well as the B2 (G2) and B3 (G3) domains of SpG. *In vitro* molecular evolution directed by human, rabbit, bovine, or goat polyclonal IgGs and four subclasses of mouse monoclonal IgGs generated one common combination, D-C-G3. A series of assays demonstrated that D-C-G3 exhibited a potential novel IgG binding property that was obviously different from those of both parent proteins. This study provides an example of successful protein engineering through *in vitro* molecular evolution and useful approaches for structure and function studies of IBPs.

Bacterial immunoglobulin (Ig)-binding proteins (IBPs) can bind to specific sites on Ig and mediate cellular pathogenicity in the host<sup>1</sup>. SpA, SpG, and protein L (from *Peptostreptococcus magnus*) are three well-defined IBPs that play important roles in the pathogenicity of bacteria. SpA is composed of 524 amino acid residues and has a molecular weight of 57 kDa. The extracellular portion of SpA consists of a tandem repeat of five highly-homologous IgG-binding domains designated (from the N terminus) E, D, A, B and C, each of which contains approximately 58 amino acid residues. The overall structures of these domains are three up-down  $\alpha$ -helixes, and all five domains of SpA exhibit Ig-binding abilities<sup>2-4</sup>. Each single-binding domain of SpA possesses similar binding characteristic of the whole protein, including high affinity for the interface between the second constant region of the heavy chain (CH2) and CH3 domains (CH2 $\gamma$ -CH3 $\gamma$ ) of IgG Fc<sup>5,6</sup>, as well as low affinity for the antigen binding fragment (Fab) of a subset of Igs, of which the heavy chain variable regions belong to human VHIII family<sup>7-9</sup>. SpG is composed of 594 amino acid residues and contains three highly-homologous Ig-binding domains identified as B1, B2 and B3<sup>10</sup>. Each domain of SpG consists of two pairs of antiparallel  $\beta$ -sheets connected by a single  $\alpha$ -helix<sup>11,12</sup>. SpG binding domains also show high affinity for the CH2 $\gamma$ -CH3 $\gamma$  interface of the IgG Fc. Additionally, SpG can bind to Fab in the first constant region of the Ig  $\gamma$  chain (CH1 $\gamma$ )<sup>13</sup>. Because of their unique antibody binding features, IBPs have fundamental applications in biological and medical sciences, such as antibody purification, antibody diagnostic detection, immunoabsorption therapy, and immunoprecipitation assays<sup>14-17</sup>.

Although each binding domain of both SpA and SpG shows high affinity for and binds several common residues at the CH2 $\gamma$ -CH3 $\gamma$  interface of IgG, these two proteins have developed different binding strategies: the interaction between SpG and IgG Fc involves mainly charged and polar contacts, whereas SpA and Fc are held together through non-specific hydrophobic and a few polar interaction<sup>18</sup>. It is also found that both heavy (two CH2 $\gamma$ -CH3 $\gamma$ s) and light chains are involved in the binding of SpA and SpG to IgG<sup>5,8</sup>. Besides, SpA and SpG exhibit apparent differences in binding to IgG classes of various species and subclasses<sup>19,20</sup>.

Some chimeric IBPs, including protein LA, protein LG and protein AG, have been constructed by combining various IBPs<sup>21-23</sup>. These chimeric IBPs preserved the binding properties of both the parent IBPs and exhibited apparent application advantages. However, no obvious novel binding properties were observed in these chimeric IBPs. Whether specific combinations of Ig-binding domains from different IBPs could produce molecules with

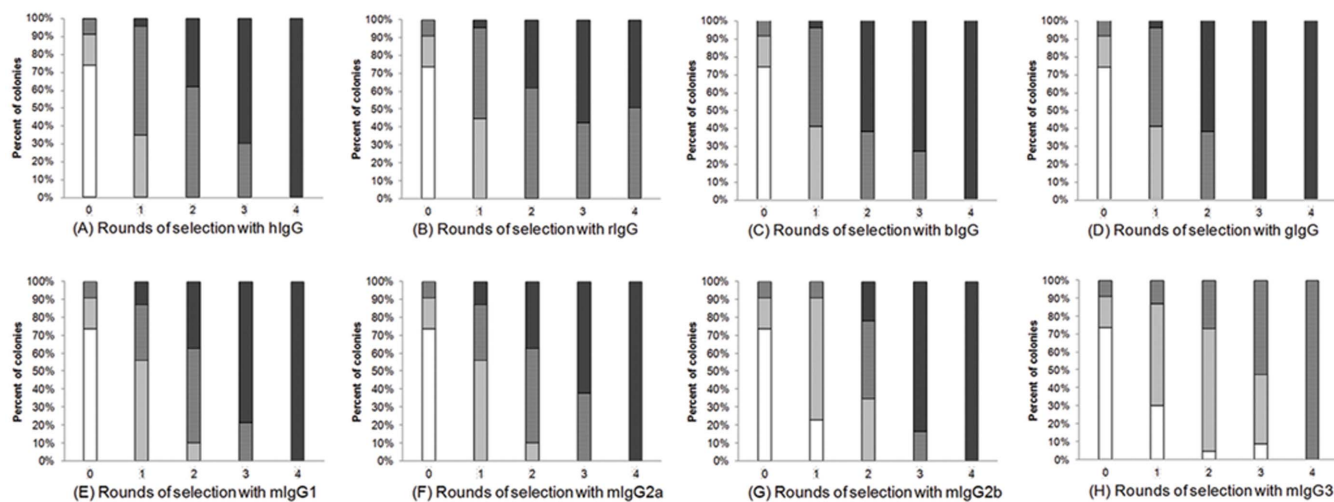


**Figure 1 | Proportion of the phage clones with different sizes of inserted fragments from the 22 phage clones after each round of selection with eight IgG molecules (A–H).** □, phage clones with no inserted fragment; ■, phage clones displaying one domain of the combinatorial Ig-binding molecules; ■, phage clones displaying two domains of the combinatorial Ig-binding molecules; ■, phage clones displaying three domains of the combinatorial Ig-binding molecules.

novel binding properties remained unclear. Our previous *in vitro* molecular evolution of combinatorial phage libraries displaying randomly-rearranged molecules of various Ig-binding domains of SpA, SpG and protein L by human Igs yielded numerous novel combinations of those domains that do not exist in natural bacterial IBPs, and these molecules are referred as newly evolved Ig-binding molecules (NEIBM) and exhibit novel Ig-binding properties<sup>24</sup>. LD5 and LD3, both of which represent one type of NEIBM, exhibited double-site binding to the VH3 and V $\kappa$  regions of human Ig Fab and had high affinity for human IgM<sup>25</sup>. Application of LD5 as conjugate was shown to enhance IgM detection in an anti-HCV ELISA assay<sup>26</sup>.

In this study, we constructed a combinatorial phage library that displayed randomly-rearranged A, B, C, D and E domains of SpA as well as G2 and G3 domains of SpG. *In vitro* molecular evolution of this library, which was directed by human IgG (hIgG), rabbit IgG (rIgG), bovine IgG (bIgG), goat IgG (gIgG) and four subclasses of mouse monoclonal antibodies mIgG1, mIgG2a, mIgG2b, and mIgG3, generated one novel common molecule D-C-G3. This new NEIBM molecule exhibits a potential novel IgG binding property to IgG.

## Results

***In vitro* molecular evolution of the phage library displaying randomly-rearranged Ig-binding domains of SpA and SpG.** We constructed a combinatorial phage library that displayed randomly-rearranged A, B, C, D and E domains from SpA as well as G2 and G3 domains of SpG, and conducted *in vitro* molecular evolution of this library using hIgG, rIgG, bIgG, gIgG, mIgG1, mIgG2a, mIgG2b or

mIgG3 as bait. As we observed in a previous phage library study<sup>24</sup>, the distribution of the inserted fragment sizes changed remarkably during the whole *in vitro* evolutions, and so did in this research (Fig. 1), indicating effective evolution. The results showed that the proportion of phage clones displaying two and three domains in the original library was less than 10%, but increased dramatically to 100% after three or four rounds of selection. Ten phage clones from each third or fourth post-selection population were then randomly chosen for sequencing analysis. To our surprise, the evolutions directed by hIgG, bIgG, gIgG, mIgG1, mIgG2a and mIgG2b yielded a common combination D-C-G3; additionally, rIgG generated two combinations D-C-G3 and D-C at the same amount, but mIgG3 only produced the combination D-C (Table 1). Interestingly, all of the D-C-G3 combinations resulted from those seven different IgG molecules displayed three identical linking peptides, ESQ between D and C, VSM between C and G3, and HQQ following G3, which indicated the strictness of these *in vitro* molecular evolutions.

**D-C-G3 exhibits a novel binding activity to IgG.** To characterise its binding properties, D-C-G3 was expressed as a fusion protein using pET-32a(+) expression vector. The control combinations of D-C and D-B yielded from a second post-selection population directed by hIgG were also expressed (Fig. 2).

ELISA analysis showed that D-C-G3 exhibited enhanced binding activity against hIgG, mIgG1, mIgG2a and mIgG2b, compared to both SpA and SpG. This protein also bound rIgG and mIgG3 with comparable binding activities as SpA, which were much stronger

**Table 1 | Sequences of the inserted fragments in the phage clones in the original library and the eight IgG bait selected libraries**

Phage Libraries	Composition of single domains of inserted fragment
The 4th round of selection with hIgG (10 *)	DESQ** <sub>-</sub> C <sub>VSM</sub> -G <sub>3</sub> HQQ (10)
The 4th round of selection with rIgG (10)	DESQ-C <sub>VSM</sub> -G <sub>3</sub> HQQ (5), DAHT-C <sub>MLS</sub> (5)
The 4th round of selection with bIgG (10)	DESQ-C <sub>VSM</sub> -G <sub>3</sub> HQQ (10)
The 3th round of selection with gIgG (10)	DESQ-C <sub>VSM</sub> -G <sub>3</sub> HQQ (10)
The 4th round of selection with mIgG1 (10)	DESQ-C <sub>VSM</sub> -G <sub>3</sub> HQQ (10)
The 4th round of selection with mIgG2a (10)	DESQ-C <sub>VSM</sub> -G <sub>3</sub> HQQ (10)
The 4th round of selection with mIgG2b (10)	DESQ-C <sub>VSM</sub> -G <sub>3</sub> HQQ (10)
The 4th round of selection with mIgG3 (10)	DAHT-C <sub>MLS</sub> (10)

\*, the number of clones randomly selected for sequencing analyses; \*\*, the random linking peptides.

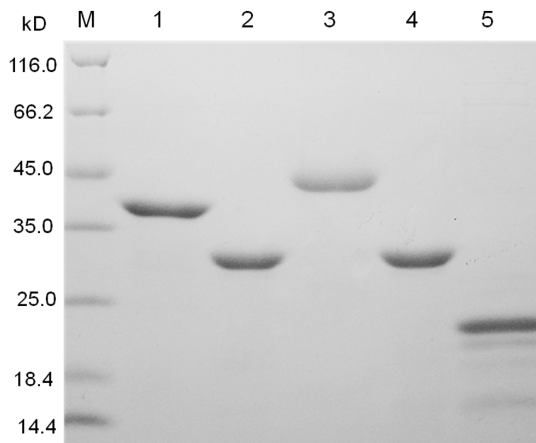


**Figure 2 |** The prokaryotic expression of SpA, SpG, D-C, D-B and D-C-G3. M, protein marker, indicating 116.0 kDa, 66.2 kDa, 45.0 kDa, 35.0 kDa, 25.0 kDa, 18.4 kDa and 14.4 kDa; lane 1, D-C-G3; lane 2, D-C; lane 3, SpA; lane 4, SpG; lane 5, PET-32A.

than that of SpG. In addition, D-C-G3 exhibited comparable binding activities to bIgG and gIgG as SpG, which was remarkably stronger than that of SpA (Fig. 3).

Dot blot assay revealed the same results as ELISA analysis did (Fig. 4B), whereas western blot analysis showed some differences. According to western blot results, D-C-G3 only consistently displayed stronger binding to mIgG2a and mIgG2b, compared to SpA and SpG (Fig. 4A). In contrast, D-C-G3, SpA and SpG could all strongly bind to hIgG and rIgG. Besides, D-C-G3 and SpA bound to mIgG1 and mIgG3 with high affinity, but SpG much lower. As for binding to bIgG and gIgG, D-C-G3 showed high affinity with both, whereas SpG weakly bound to the former Ig and strongly to the latter. However, SpA showed no obvious binding to either bIgG or gIgG.

To further characterise the binding properties of D-C-G3, competitive inhibition experiments were conducted. As shown in

Figure 5, competitive binding of D-C-G3, SpA and SpG to hIgG, mIgG1, mIgG2a and mIgG2b were examined, and it was found that D-C-G3 exhibited a much stronger inhibitory potential than both SpA and SpG, demonstrating its obviously enhanced binding activities to these IgGs; for the binding of D-C-G3, SpA and SpG to rIgG and mIgG3, D-C-G3 exhibited an inhibitory potential equivalent to SpA, which was stronger than that of SpG. As to the binding to bIgG and gIgG, the results showed that D-C-G3 exhibited an inhibitory potential at a similar level as SpG, but much stronger than SpA. The binding properties of D-C-G3 characterised by competitive inhibition experiments were consistent with the results of ELISA and dot blot assays.

**D-C-G3 showed selective IgG binding enhancement.** To make a quantitative assessment of the binding properties of D-C-G3 relative to SpA, SpG or D-C, their interactions with hIgG, rIgG, gIgG, mIgG1, mIgG2a, mIgG2b or mIgG3 were analyzed by Surface Plasmon Resonance (SPR). Basically consistent with ELISA analysis, SPR data (Table 2) showed that compared to D-C and SpA, D-C-G3 exhibited enhanced binding activity to a different degree against all tested IgGs except rIgG, and compared to SpG, higher binding activity of D-C-G3 was observed against all IgGs but not for gIgG. Interestingly, the affinity constants of D-C-G3 interacting with hIgG, gIgG and mIgG2a, which have one or none amino acid variation in the SpG binding sites of CH1 $\gamma$  chain (Figure 6), are at least 21 times and 16 times more than that of D-C and SpA respectively. In contrast, when interacting with mIgG3 and rIgG, which have three or more variations (Figure 6), the affinity constants of D-C-G3 are at most 2.04 and 1.78 times more than that of D-C and SpA respectively.

**D-C-G3 improved the purification of monoclonal and polyclonal antibodies.** To investigate whether D-C-G3 has the application advantage in antibodies purification, we compared the purification efficiency of affinity chromatography columns made from D-C-G3, SpA or SpG. Four kinds of monoclonal antibodies ascites, human serum and rabbit serum were used in the study for antibody

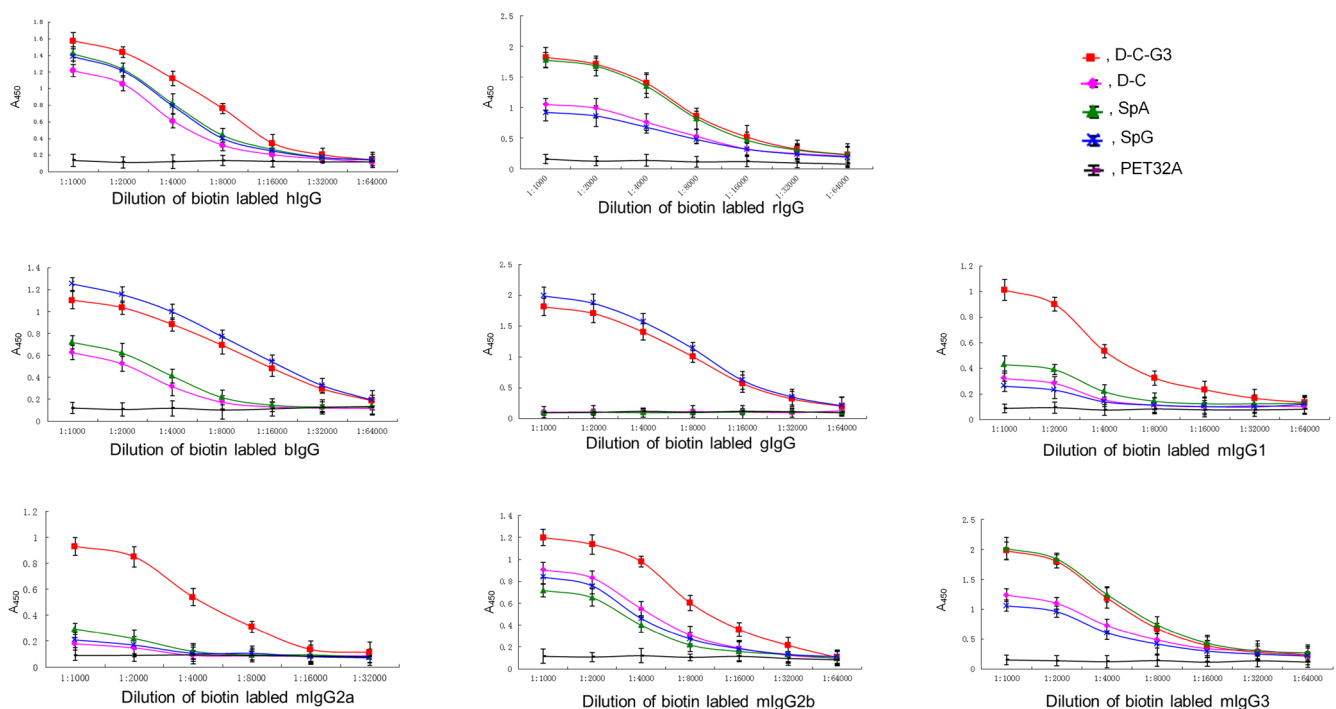


**Figure 3 |** Binding activities of D-C-G3 to hIgG, rIgG, bIgG, gIgG and four subclasses of monoclonal mIgG compared to D-C, D-B, SpA and SpG according to ELISA analysis. ■, D-C-G3; ●, D-C; ▲, SpA; ✕, SpG; -, PET-32A control protein.

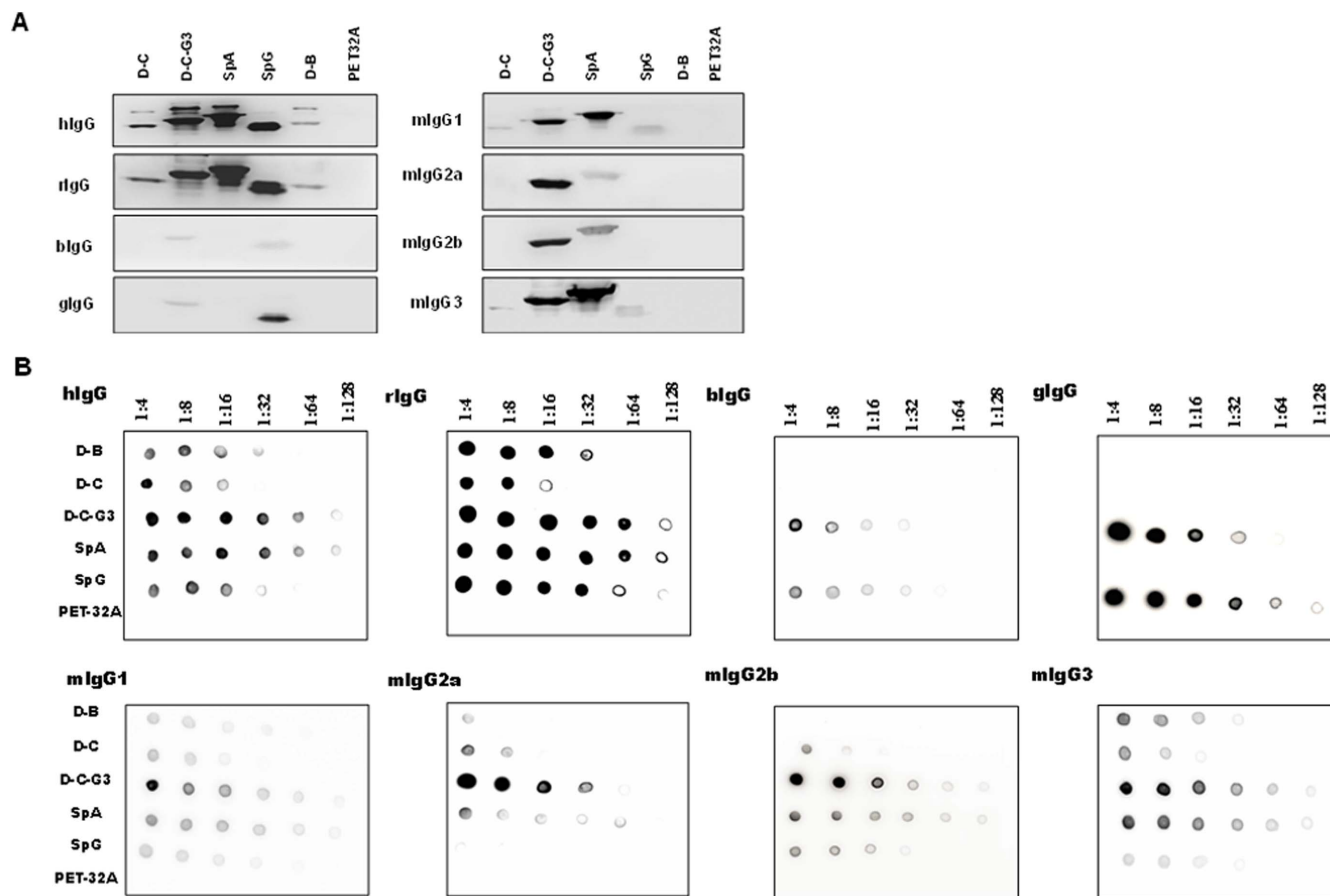


**Figure 4** | Binding activities of D-C-G3 to hIgG, rIgG, bIgG, gIgG and four subclasses of monoclonal mIgG compared to D-C, D-B, SpA and SpG according to western blot (A) and dot blot analyses (B). Western blot results (A) are representative cropped images and every set have been processed under similar conditions as detailed in the methods section.

purification. As shown in Figure 7, D-C-G3 affinity column recovered much greater amount of mIgG2a, mIgG2b mIgG1 monoclonal antibodies from ascites and polyclonal antibodies from human serum than that by SpA and SpG affinity chromatography. Additionally, D-C-G3 and SpA showed similar efficiency in rIgG and mIgG3 purifications. The data indicates that D-C-G3 has some advantages in some types of antibodies' purification, and therefore has application potential.

## Discussion

In this study, our *in vitro* molecular evolution directed by various IgGs generated a common combination, D-C-G3, which exhibited novel IgG-binding features, compared to the parent IBPs, SpA and SpG. This result was not initially expected. It is known that both SpA and SpG contain tandem repeats of multiple highly-homologous IgG-binding domains, and these tandem repeats can produce intramolecular binding avidity and display selective advantages in molecular evolution<sup>8</sup>. As each IgG molecule consists of two identical Ig  $\gamma$  chains, it serves as an ideal target for simultaneous two-site intramolecular binding. Theoretically, IgG molecules of different animals or subclasses are supposed to be different targets for variable combinations of SpA and/or SpG binding domains, and have specific two-site intramolecular binding activity. The design of the phage library, which randomly-rearranged the SpA and SpG binding domains, guaranteed the diversity and randomness of the original library combinations, as well as the final "winners" with advantages of binding to each kind of IgG bait after strict evolutions. To our surprise, the *in vitro* molecular evolutions of this library directed by hIgG, bIgG, gIgG, mIgG1, mIgG2a and mIgG2b did not generate as

many combinations of IgG-binding domains as expected, and only one common combination D-C-G3 (Table 1) was produced. Although the exact mechanism for this phenomenon is unknown, it is apparent that novel D-C-G3 possessed characteristic IgG-binding activity. A possible explanation could be that the IgG molecules of different animals or subclasses might provide similar binding interfaces at their Fcs, and the binding avidity generated by D-C combination outweighs those of other combinations with these interfaces in the condition of our experiment. Consistent with this explanation, the *in vitro* molecular evolution of this library directed by four human IgG subclasses yielded a common combination, D-C<sup>27</sup>.

ELISA, dot blot and competitive ELISA analyses consistently demonstrated that D-C-G3 exhibited a remarkably enhanced binding potential to hIgG, mIgG1, mIgG2a and mIgG2b, compared to native SpA and/or SpG (Fig. 3–5). Consistent with this binding advantage, D-C-G3 was the predominant molecular during the *in vitro* molecular evolutions directed by hIgG, mIgG1, mIgG2a and mIgG2b. But for rIgG and mIgG3, D-C-G3 exhibited a binding ability equivalent to SpA (Fig. 3–5), which was much stronger than that of SpG. Both rIgG and mIgG3 directed evolutions led to D-C, the combination with both Ig-binding domains from SpA, which might have a replicative advantage during library evolution. However, rIgG directed evolution yielded the same amount of D-C and D-C-G3 combinations (Table 1), suggesting a weak binding advantage of D-C-G3 to rIgG, compared to mIgG3. Consistently, rIgG showed less amino acid variations in its SpG binding sites in the CH1 region than mIgG3 (Fig. 6). The difference might suggest that the *in vitro* molecular evolutions were affected by minor binding differences, which could not be distinguished by ELISA, dot blot or competitive

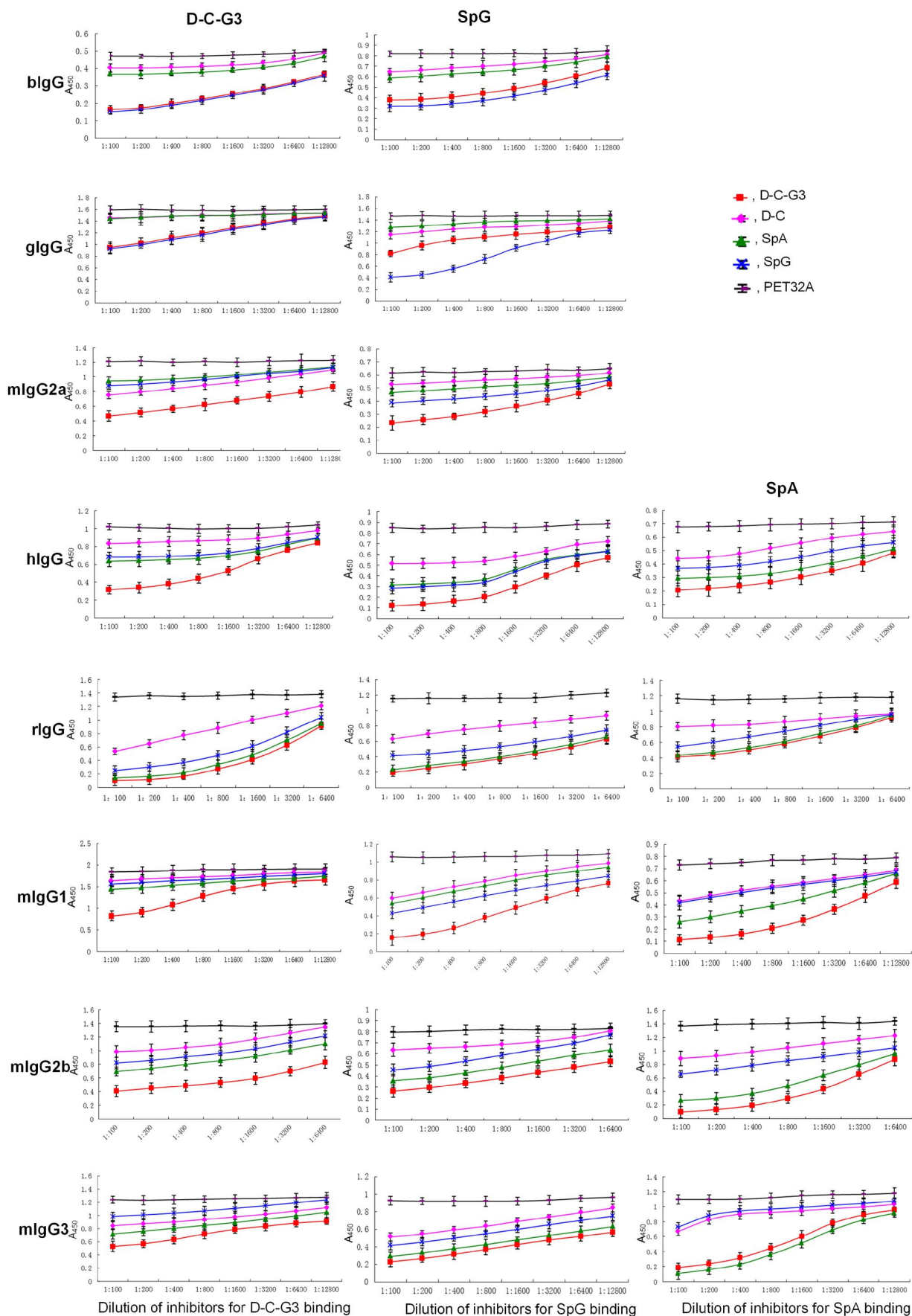


**Figure 5** | Comparison of the inhibitory potentials of D-C-G3, SpA and SpG on the binding of hIgG, rIgG, blgG, gIgG and four subclasses of monoclonal mlgG to D-C-G3, SpA and SpG according to ELISA analysis. ■, D-C-G3; ●, D-C; ▲, SpA; ✱, SpG; ▾, PET-32A control protein. The inhibition of the binding of SpA to bIgG, gIgG and mlgG2a was not shown, as the binding activities of SpA were too weak to be inhibited.



**Table 2 |** Surface plasmon resonance analysis of the interactions between D-C-G3, SpA, SpG or D-C and hIgG, rIgG, gIgG, mIgG1, mIgG2a, mIgG2b or mIgG3

Ligand	Constant	Analyte						
		mIgG1	mIgG2a	mIgG2b	mIgG3	Human IgG	Rabbit IgG	Goat IgG
DCG3	$ka(M^{-1}s^{-1})$	$1.318 \times 10^5$	$1.445 \times 10^6$	$2.168 \times 10^5$	$3.364 \times 10^5$	$1.318 \times 10^6$	$4.132 \times 10^5$	$3.147 \times 10^5$
	$kd(s^{-1})$	$1.923 \times 10^{-4}$	$1.444 \times 10^{-5}$	$1.389 \times 10^{-4}$	$1.511 \times 10^{-4}$	$8.790 \times 10^{-7}$	$2.377 \times 10^{-5}$	$6.520 \times 10^{-5}$
	$KA(M^{-1})$	$6.85 \times 10^8$	$1.00 \times 10^{11}$	$1.56 \times 10^9$	$2.23 \times 10^9$	$1.50 \times 10^{12}$	$1.74 \times 10^{10}$	$4.83 \times 10^9$
DC	$ka(M^{-1}s^{-1})$	$3.474 \times 10^4$	$1.554 \times 10^6$	$6.789 \times 10^4$	$6.783 \times 10^5$	$1.161 \times 10^6$	$6.118 \times 10^5$	$1.238 \times 10^5$
	$kd(s^{-1})$	$4.283 \times 10^{-4}$	$5.696 \times 10^{-4}$	$3.890 \times 10^{-4}$	$5.378 \times 10^{-4}$	$2.762 \times 10^{-5}$	$1.069 \times 10^{-4}$	$5.662 \times 10^{-4}$
	$KA(M^{-1})$	$8.11 \times 10^7$	$2.73 \times 10^9$	$1.75 \times 10^8$	$1.26 \times 10^9$	$4.20 \times 10^{10}$	$5.72 \times 10^9$	$2.19 \times 10^8$
SpA	$ka(M^{-1}s^{-1})$	$6.034 \times 10^4$	$1.531 \times 10^6$	$1.142 \times 10^5$	$2.516 \times 10^5$	$9.63 \times 10^5$	$6.470 \times 10^5$	$1.295 \times 10^5$
	$kd(s^{-1})$	$3.698 \times 10^{-4}$	$3.155 \times 10^{-4}$	$3.578 \times 10^{-4}$	$3.142 \times 10^{-4}$	$1.156 \times 10^{-5}$	$2.300 \times 10^{-5}$	$8.497 \times 10^{-4}$
	$KA(M^{-1})$	$1.63 \times 10^8$	$4.85 \times 10^9$	$3.19 \times 10^8$	$8.01 \times 10^8$	$8.34 \times 10^{10}$	$2.81 \times 10^{10}$	$1.52 \times 10^8$
SpG	$ka(M^{-1}s^{-1})$	$9.295 \times 10^4$	$1.089 \times 10^6$	$1.212 \times 10^5$	$2.346 \times 10^5$	$1.747 \times 10^6$	$1.240 \times 10^6$	$7.160 \times 10^5$
	$kd(s^{-1})$	$7.426 \times 10^{-4}$	$5.762 \times 10^{-4}$	$5.983 \times 10^{-4}$	$4.723 \times 10^{-4}$	$2.615 \times 10^{-5}$	$3.190 \times 10^{-5}$	$1.243 \times 10^4$
	$KA(M^{-1})$	$1.25 \times 10^8$	$1.89 \times 10^9$	$2.03 \times 10^8$	$4.97 \times 10^8$	$6.68 \times 10^{10}$	$3.88 \times 10^{10}$	$5.76 \times 10^9$
$KA_{DCG3}/KA_{DC}$	8.45	36.64	8.94	1.76	35.70	3.04	22.26	
$KA_{DCG3}/KA_{SpA}$	4.20	20.6	4.90	2.78	17.99	0.62	31.69	

ELISA assays (Fig. 3–5). For bIgG and gIgG, D-C-G3 exhibited an equivalent binding ability to that of SpG, but much stronger than SpA (Fig. 3–5). The evolutions directed by these two IgG baits only generated D-C-G3 but no combinations with all domains from SpG. One possible explanation for this is that D-C-G3 exhibited a comprehensive selection advantage by balancing both the binding and replicative advantages. Each of the five SpA domains, E, D, A, B, and C as well as the two SpG domains, G2 and G3, were used as building blocks for the construction of the phage library to produce various random combinations of these domains. Obviously, D-C-G3 could be easily reproduced compared to the combinations of three tandem repeats of the SpG domains. Taken together, the results of our *in vitro* evolutions are basically consistent with the binding properties of D-C-G3, the SpA binding domains and the SpG binding domains.

All of the binding assays in this study demonstrated substantially enhanced binding activity of D-C-G3 to most of the tested IgGs. How this binding enhancement was achieved is an interesting topic. It is known that both SpA and SpG binding domains can bind to the CH2 $\gamma$ -CH3 $\gamma$  interface region through two-site intramolecular

binding avidity<sup>11,12</sup>. Besides, the SpA binding domains can bind to the variable region of the heavy chains belonging to the human VHIII family<sup>19,28–30</sup>, and SpG can bind to the first constant region of the Ig $\gamma$  chain (CH1 $\gamma$ )<sup>11,12</sup>. Because D-C-G3 has three tandem repeats of binding domains, a simultaneous tri-site binding mode might properly account for this binding enhancement. Theoretically, D-C-G3 could produce two types of tri-site binding modes involving two binding sites located at CH2 $\gamma$ -CH3 $\gamma$ s and the third at CH1 $\gamma$  or VHIII. In Figure 6, it is very interesting to find that the sequence variations of the SpG binding amino acids in CH1 $\gamma$  of various IgG molecules are highly consistent with the IgG-binding enhancement of D-C-G3: hIgG, mIgG1, mIgG2a, mIgG2b, bIgG and gIgG have less than three amino acid variations in the eight amino acids involved in SpG binding in CH1 $\gamma$ , and show remarkable binding enhancement with D-C-G3; rIgG and mIgG3 have more than four amino acid variations, and exhibit little binding enhancement with D-C-G3 (Fig. 3–5, Table 2). This finding supports the tri-site model, in which D-C binds to two CH2 $\gamma$ -CH3 $\gamma$ s and G3 binds to CH1 $\gamma$ , representing a novel binding mode.

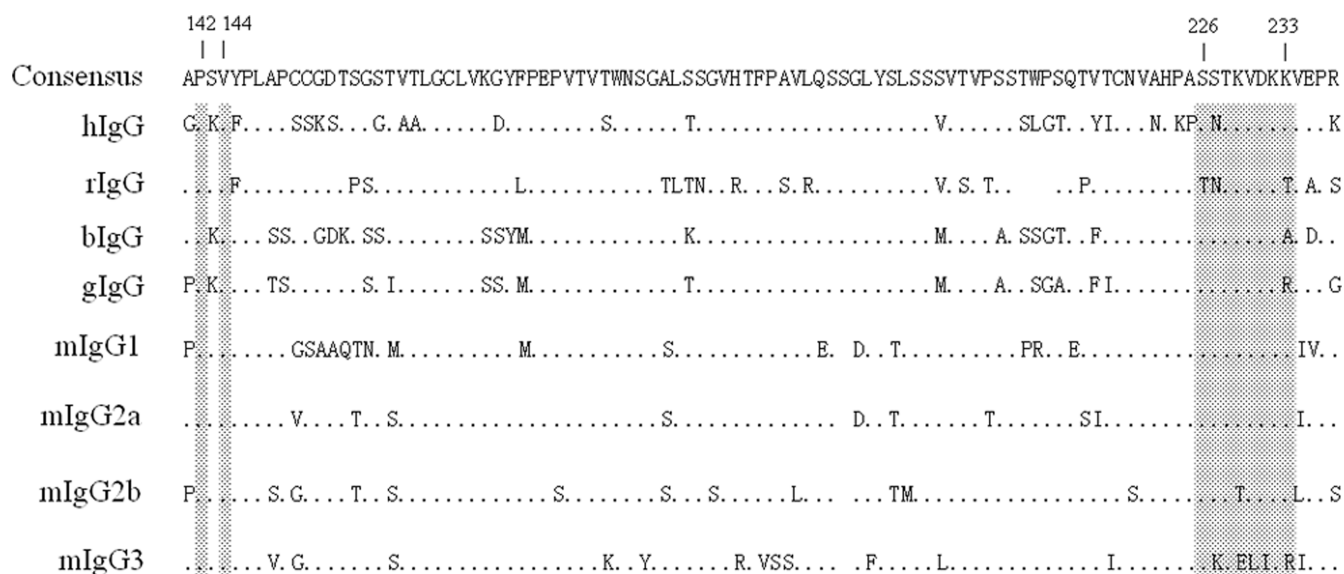


**Figure 6 |** Sequence comparison of the SpG binding sites in the CH1  $\gamma$  chain of these eight IgG molecules. The sequences of bIgG CH1 (GenBank: ABE68619.1), hIgG CH1 (GenBank: AAA02914.1), rIgG CH1 (GenBank: AAB59265.1), gIgG CH1 (GenBank: AAX45026.1), mIgG1 CH1 (GenBank: CAD32497.1), mIgG2a CH1 (GenBank: BAA11361.1), mIgG2b CH1 (GenBank: BAA11359.1) and mIgG3 CH1 (GenBank: AAB59697.1) were aligned. The shaded sequences represent the binding sites to SpG<sup>34</sup>. \*, No. 142 amino acid residue in mouse immunoglobulin gamma 1 heavy chain.

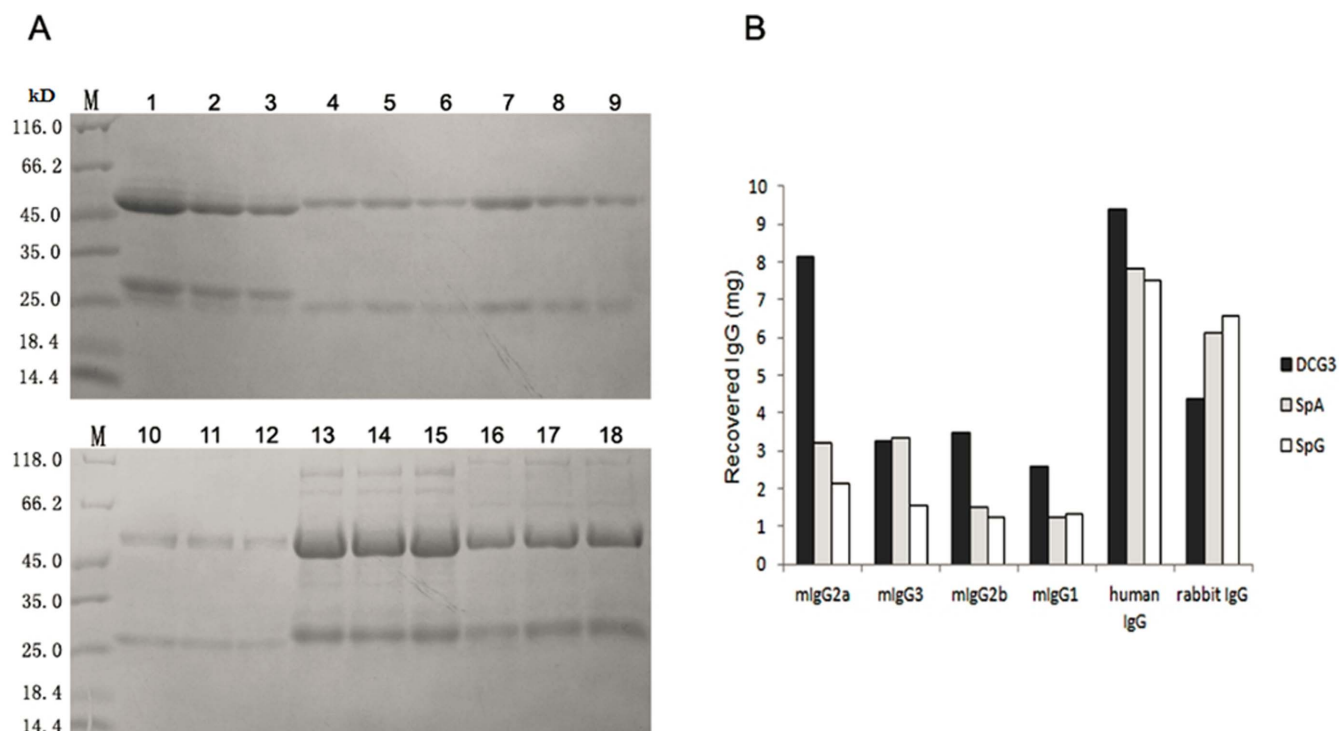


**Figure 7 | Comparison of IgG purification from mouse monoclonal ascites, human serum and rabbit serum with D-C-G3, SpA and SpG affinity chromatography.** (A) SDS/PAGE analysis of different IgG purified by D-C-G3, SpA and SpG affinity chromatography. M, protein molecular weight marker; 1–3, mIgG2a purified by DCG3, SpA, SpG affinity chromatography, respectively; 4–6, mIgG3; 7–9, mIgG2b; 10–12, mIgG1; 13–15 human IgG; 16–18, goat IgG purified by DCG3, SpA, SpG affinity chromatography, respectively. (B) Recovery of IgG from monoclonal antibodies, human serum and rabbit serum purified by different affinity chromatography. Black bars, purified IgG with DCG3 affinity chromatography; grey bars, purified IgG with SpA affinity chromatography; white bars, purified IgG with SpG affinity chromatography.

SpA had a higher affinity than SpG to bind polyclonal IgGs from human and mouse, while SpG showed stronger interaction with polyclonal IgGs from bovine, goat and sheep<sup>31</sup>. Furthermore, the binding of SpG to CH2-CH3 interface region with a two sites model has a binding constant of  $6 \times 10^9$ , which is 15 times larger than that of SpG with human IgG Fab at the CH1<sup>5</sup>. Thus in tri-site binding mode of D-C-G3 and IgG, D-C should present strong binding to CH2 $\gamma$ -CH3 $\gamma$  with a model of two sites binding, and G3 only provides additional one-site weaker binding for CH1 than that for CH2-CH3 domain interface. The SPR data showed that D-C exhibited the same level of affinity constants to all tested IgGs as SpA (Table 2), indicating their two sites binding to CH2 $\gamma$ -CH3 $\gamma$ <sup>11,12</sup>. The affinity constants of D-C-G3 interacting with hIgG, gIgG and mIgG2a are much more than (over 16 times) that of D-C and SpA, suggesting an effective tri-site binding to CH2 $\gamma$ -CH3 $\gamma$ s and CH1 $\gamma$ . Furthermore, the affinity constants of D-C-G3 with mIgG1 and mIgG2b, which are 8.45 and 8.94 times of that for D-C respectively, probably imply an incomplete tri-site binding.

We previously demonstrated that the NEIBM LD5, which exhibited a novel binding property of double site binding to the VH3 and VK regions of human Ig Fab, enhanced the detection of IgM in an anti-HCV ELISA assay<sup>25,26</sup>. In this study, with the novel tri-site binding mode, enhanced binding activity of D-C-G3 to hIgG might have potential application in IgG detection for the diagnosis of infections caused by various pathogens. Interestingly, D-C-G3 exhibited strong binding potential to all subclasses of mouse monoclonal antibodies, whereas SpA only exhibited a strong binding to mIgG3, and SpG did not strongly bind to any subclass of mouse monoclonal antibodies. These enhanced binding activities meant that D-C-G3 might be useful for either the purification of mouse monoclonal antibodies by affinity chromatography or precipitation assays using these antibodies. In this work, D-C-G3 affinity chromatography (Figure 7)

showed remarkably enhanced yields in the purification of mIgG2a, mIgG2b, mIgG1 monoclonal antibodies and human polyclonal antibodies compared with SpA or SpG affinity chromatography.

Under the denaturing conditions of the western blot analysis, only the enhanced binding potential of D-C-G3 to mIgG2a and mIgG2b were preserved, whereas its enhanced binding ability to hIgG, rIgG, mIgG1 and mIgG3 were greatly attenuated (Fig. 4A). This phenomenon could be reasonably attributed to the poor stability of the D-C-G3 molecule, which was artificially produced by *in vitro* molecular evolution, compared with the natural SpA and SpG molecules. This finding suggests the complexity in creating useful artificial proteins by protein engineering.

In brief, we obtained a novel NEIBM, D-C-G3, by *in vitro* molecular evolution, and this molecule showed a potential novel enhanced IgG binding property, compared to its parent proteins, SpA and SpG. This protein can promote the purification efficiency of some mouse monoclonal antibodies or polyclonal antibodies, and might have potential applications in a variety of fields. In addition, our study provides an example of successful protein engineering through *in vitro* molecular evolution and presents a useful approach for the study of the structure and function of IBPs.

## Methods

**Oligonucleotides, vectors and reagents.** Primers were custom synthesized by Sangon Biological Engineering Technology (Shanghai, China). The phagemid vector pCANTAB5S was constructed by inserting the Xba I-Stu I-Sal I-Kpn I-(Gly4Ser)<sub>3</sub> DNA fragment into the pCANTAB5L vector (Pharmacia Biotech, Uppsala, Sweden) between the Sfi I and Not I restriction sites<sup>32</sup>. The encoding sequence of SpA was inserted into pCANTAB5S using the Xba I site. The phagemid pCANTAB5S-SpA, which contains five mono-domain DNA fragments, E, D, A, B and C (GenBank: P02976), as well as two plasmids, pMD-18T-G2 and pMD-18T-G3, which included the B2 and B3 sequences of SpG, respectively (GenBank: P06654), were constructed by our lab. Helper phage M13K07 was purchased from Pharmacia Biotech, Uppsala, Sweden. SpA was kindly provided by Shanghai Fudan-Zhangjiang Bio-



Table 3 | Primers for the amplification of DNA fragments encoding the Ig-binding single domains of SpA and SpG

Name	Description	Primer sequence (5'–3')
UA	Sense terminal primer of A	TCGTCAGACGCCGTACCTGCTCTAGA*GCTGACAACAATTCAAC
UD	Sense terminal primer of D	TCGTCAGACGCCGTACCTGCTCTAGA*GCTGATGCGCAACAAAAT
DA/D	Antisense random primer of A/D	TCGTCAGACGCCGTACCTGCTCTAGA*SNNSNNSNN**TTTCGGTGCTTGAGATTG
UB	Sense terminal primer of B	TCGTCAGACGCCGTACCTGCTCTAGA*GCGGATAACAAAATTCAAC
DB	Antisense random primer of B	TCGTCAGACGCCGTACCTGCTCTAGA*SNNSNNSNN**TTTTGGTGCTTGATC
UC	Sense terminal primer of C	TCGTCAGACGCCGTACCTGCTCTAGA*GCTGACAACAATTCAAC
DC	Antisense random primer of C	TCGTCAGACGCCGTACCTGCTCTAGA*SNNSNNSNN**TTTTGGTGCTTGAGCATC
UE	Sense terminal primer of E	TCGTCAGACGCCGTACCTGCTCTAGA*GCTCAACAAAATGCTT
DE	Antisense random primer of E	TCGTCAGACGCCGTACCTGCTCTAGA*SNNSNNSNN**TTTTGGAGCTTGAGAGTC
UG2/G3	Sense terminal primer of G2/G3	TCGTCAGACGCCGTACCTGCTCTAGA*ACCTACAAACTGGTATC
DG2/G3	Antisense random primer of G2/G3	TCGTCAGACGCCGTACCTGCTCTAGA*SNNSNNSNN**TTCGGTAACGGTGAAGGT
Sec	Secondary amplifying of A, B, C, D, E, G2/G3	ATACCTAGCCCATTACCCTAGCCACCTAGTCCGTCGTCAGACGCCGTACCTGCTCTAGA*
P1	Primer located in the upward of the cloning site of pCANTAB5S	CAACGTGAAAAAATTATTAT CGC
P2	Primer located in the downward of the cloning site of pCANTAB5S	GTAATGAATTTTCTGTATGAGG

\*, Xba I restriction sites are in italics; \*\*, nucleotide sequences of the random linking peptides are underlined (N = A/T/C/G, S = G/C).

Pharmaceutical Co. Ltd, Shanghai, China, and SpG was obtained from Bosters Biological Engineering Technology (Wuhan, Hubei, China). The prokaryotic expression vector pET-32a(+) was purchased from the Novagen Company (Merck KGaA, Darmstadt, Hesse, Germany) and purified using a Ni-NTA column (Amersham Pharmacia Biotech, Piscataway, NJ, USA) in our lab. hIgG, rIgG, bIgG, gIgG and horseradish peroxidase (HRP)-conjugated streptavidin were purchased from Sigma (St. Louis, MO, USA). Monoclonal anti-HCV core protein mouse antibodies 10C1, 6A3, 9H7 and 1G7 were produced in our lab and were determined to be from the mIgG1, mIgG2a, mIgG2b and mIgG3 subclasses, respectively, using purified goat anti-mouse IgG subclass-specific reagents (Southern Biotechnology Associates, Birmingham, Ala., USA). All antibodies were biotinylated using biotinyl-N-hydroxy-succinimide (Pierce, Rockford, IL, USA).

**Construction of the combinatorial phage library.** The in vitro molecular evolution of the library was previously described<sup>24,33</sup>. Gene fragments encoding the A, B, C, D and E domains of SpA as well as the G2 and G3 domains of SpG were individually generated by PCR amplification using primers listed in Table 3, which introduced Xba I restriction sites at both ends of the fragments and a nucleoside acid sequence at the 3'-end; this sequence encoded a random linking peptide 3 amino acids in length. Then, the PCR products were digested with Xba I and ligated into the Xba I site of the phagemid pCANTAB5S to construct a phage displayed random combinatorial library. The library had  $8.2 \times 10^6$  members, and the titre of the phage library was calculated to be  $1.3 \times 10^{12}$  transformation unit (TU)/ml. The host bacterial strain TG1 was purchased from Stratagene (NYSE: A, Cambridge, England). Primers P1 and P2, which were located upward and downward of the cloning site of the pCANTAB5S vector, were used to amplify the inserted fragment from the positive phages and to perform sequencing analysis of the inserted fragment.

**In vitro molecular evolution of the library.** The in vitro molecular evolution of the library was previously described<sup>24,33</sup>. Enzyme linked immunosorbent assay (ELISA) plates (Nunc, Roskilde, Denmark) were coated with hIgG, rIgG, bIgG, gIgG, mIgG1, mIgG2a, mIgG2b and mIgG3, and the library of approximately of  $1 \times 10^{12}$  transforming units (TUs) per well was added for evolutionary selection. Twenty-two phage clones were randomly chosen after each round of selection to test the presence of the inserted DNA fragments by PCR using the P1 and P2 primers to detect the distribution of various fragment sizes displayed by phage library and post-selections. The phagemid pCANTAB5S was used as a negative control. Ten phage clones in the last round of the post-selection libraries were picked randomly and sequenced. The multiple sequence alignment was analyzed using the DNASTAR software package.

**Production and purification of representative combinations.** The representative phagemid inserts containing D-C-G3 or D-C<sup>27</sup> were amplified by PCR. The amplified DNA were cloned between the Nco I and Sac I sites of pET-32a(+) expression vector. The recombinant plasmids were subsequently transformed into Escherichia coli BL21 (DE3) cells for the production of the proteins, and a Ni-NTA column was used to purify the target proteins according to the manufacturer's instructions (Qiagen, Germany).

**ELISA and competitive inhibition ELISA.** To perform the ELISA test, purified D-C-G3, D-C, SpA and SpG were coated at a concentration of 1 µg per well and then incubated with serially diluted (1 : 2) biotin-labelled hIgG, rIgG, bIgG, gIgG, mIgG1, mIgG2a, mIgG2b or mIgG3 from an initial concentration of 1 µM. The reactive complexes were detected using 2 µg/ml HRP-conjugated streptavidin. For the competitive inhibition assays, D-C-G3, D-C, SpA and SpG proteins were serially

diluted (1 : 2) from an initial concentration of 1 µM, and 0.1 µM biotin-labelled hIgG, rIgG, bIgG, gIgG, mIgG1, mIgG2a, mIgG2b or mIgG3 was added to ELISA plates pre-coated with D-C-G3, SpA or SpG. The reactive complexes were detected using HRP-conjugated streptavidin. PET-32A was used as a negative control.

**Western blot and dot blot assays.** Western blot analysis for the tested D-C-G3, D-C, SpA and SpG proteins were separated with biotin-labelled hIgG, rIgG, bIgG, gIgG, mIgG1, mIgG2a, mIgG2b and mIgG3 as described previously<sup>25</sup>. For the dot blot analysis<sup>33</sup>, two micrograms of D-B, D-C, D-C-G3, SpA, and SpG were spotted onto nitrocellulose membranes in serial doubling dilutions (initial 1 : 4 dilution) for the dot blot assay. PET-32A was used as a negative control.

**Biosensor analyses.** The binding properties of D-C-G3, D-C, SpA or SpG to hIgG, rIgG, gIgG, mIgG1, mIgG2a, mIgG2b and mIgG3 were studied by surface plasmon resonance (SPR) using a Biacore T100 instrument (Biacore, GE, USA). Briefly, D-C-G3, D-C, SpA or SpG (diluted in 10 mM sodium acetate, pH 5.0, 5.0, 5.0, or 4.0) was coupled to CM-5 sensor chips using amine-coupling chemistry according to the manufacturer's instructions. Binding experiments were performed with serial 1 : 2 dilutions of the analytes with the initial concentrations of hIgG, rIgG, gIgG, mIgG1, mIgG2a, mIgG2b and mIgG3 at 1 µg/ml, 2 µg/ml, 10 µg/ml, 20 µg/ml, 2 µg/ml, 20 µg/ml and 20 µg/ml respectively. The association and dissociation were measured at a flow rate of 30 µl/min, using NaCl/HEPES supplemented with 0.005% surfactant P20 as flow buffer. The sensor-chip surfaces were regenerated with 100 mM alanine-HCl (pH 2.0). KA, affinity constant, was calculated as,  $KA = ka$  (association rate constant)/kd (dissociation rate constant).

**Affinity chromatography.** Thirty milligrams of the D-C-G3 fusion proteins were immobilised onto 3 ml Sepharose column according to the manufacturer's instructions (Amersham, Uppsala, Sweden). Three millilitres of unconditioned mouse ascites and two millilitres of human serum or goat serum were 1 : 8 diluted in PBS respectively, and applied onto the 3ml D-C-G3 coupled-column, SpA or SpG coupled-column (Amersham Pharmacia Biotech AB, Uppsala, Sweden) at room temperature. After extensive washing with PBS (pH 7.0), the bound proteins were eluted with 100mM sodium acetate (pH 3.0); about four millilitres of eluted proteins were collected for each IgG and dialyzed against PBS (pH 7.0). Ten microliter eluted proteins were analyzed by 12% SDS/PAGE under reducing conditions. In addition, quantification of the eluted proteins was determined by Bradford assay.

**Data analysis.** All experiments were independently performed at least three times in triplicate. The data are presented as the mean ± S.E. and were analyzed with an ANOVA or Student's t-test. A P value < 0.05 was considered significant.

- Kronvall, G. & Jonsson, K. Receptins: a novel term for an expanding spectrum of natural and engineered microbial proteins with binding properties for mammalian proteins. *J Mol Recognit* **12**, 38–44 (1999).
- Uhlen, M. *et al.* Complete sequence of the staphylococcal gene encoding protein A. A gene evolved through multiple duplications. *J Biol Chem* **259**, 1695–1702 (1984).
- Moks, T. *et al.* Staphylococcal protein A consists of five IgG-binding domains. *Eur J Biochem* **156**, 637–643 (1986).
- Gouda, H. *et al.* Three-dimensional solution structure of the B domain of staphylococcal protein A: comparisons of the solution and crystal structures. *Biochemistry* **31**, 9665–9672 (1992).





5. Stone, G. C. *et al.* The Fc binding site for streptococcal protein G is in the C gamma 2-C gamma 3 interface region of IgG and is related to the sites that bind staphylococcal protein A and human rheumatoid factors. *J Immunol* **143**, 565–570 (1989).
6. DeLano, W. L., Ultsch, M. H., de Vos, A. M. & Wells, J. A. Convergent solutions to binding at a protein-protein interface. *Science* **287**, 1279–1283 (2000).
7. Sasso, E. H., Silverman, G. J. & Mannik, M. Human IgA and IgG F(ab')<sub>2</sub> that bind to staphylococcal protein A belong to the VHIII subgroup. *J Immunol* **147**, 1877–1883 (1991).
8. Ljungberg, U. K. *et al.* The interaction between different domains of staphylococcal protein A and human polyclonal IgG, IgA, IgM and F(ab')<sub>2</sub>: separation of affinity from specificity. *Mol Immunol* **30**, 1279–1285 (1993).
9. Graille, M. *et al.* Crystal structure of a Staphylococcus aureus protein A domain complexed with the Fab fragment of a human IgM antibody: structural basis for recognition of B-cell receptors and superantigen activity. *Proc Natl Acad Sci U S A* **97**, 5399–5404 (2000).
10. Fahnestock, S. R., Alexander, P., Nagle, J. & Filpula, D. Gene for an immunoglobulin-binding protein from a group G streptococcus. *J Bacteriol* **167**, 870–880 (1986).
11. Achari, A. *et al.* 1.67-Å X-ray structure of the B2 immunoglobulin-binding domain of streptococcal protein G and comparison to the NMR structure of the B1 domain. *Biochemistry* **31**, 10449–10457 (1992).
12. Gronenborn, A. M. *et al.* A novel, highly stable fold of the immunoglobulin binding domain of streptococcal protein G. *Science* **253**, 657–661 (1991).
13. Lian, L. Y., Barsukov, I. L., Derrick, J. P. & Roberts, G. C. Mapping the interactions between streptococcal protein G and the Fab fragment of IgG in solution. *Nat Struct Biol* **1**, 355–357 (1994).
14. Hober, S., Nord, K. & Linhult, M. Protein A chromatography for antibody purification. *J Chromatogr B Analyt Technol Biomed Life Sci* **848**, 40–47 (2007).
15. Bhullar, S. S. *et al.* Protein A-based ELISA: its evaluation in the diagnosis of herpes simplex encephalitis. *Viral Immunol* **24**, 341–346 (2011).
16. Poullin, P. *et al.* Protein A-immunoabsorption (Prosorba column) in the treatment of rheumatoid arthritis. *Joint Bone Spine* **72**, 101–103 (2005).
17. Dickson, C. Protein techniques: immunoprecipitation, in vitro kinase assays, and Western blotting. *Methods Mol Biol* **461** (2008).
18. Sauer-Eriksson, A. E., Kleywegt, G. J., Uhlen, M. & Jones, T. A. Crystal structure of the C2 fragment of streptococcal protein G in complex with the Fc domain of human IgG. *Structure* **3**, 265–278 (1995).
19. Langone, J. J. Protein A of Staphylococcus aureus and related immunoglobulin receptors produced by streptococci and pneumococci. *Adv Immunol* **32**, 157–252 (1982).
20. Akerstrom, B., Brodin, T., Reis, K. & Bjorck, L. Protein G: a powerful tool for binding and detection of monoclonal and polyclonal antibodies. *J Immunol* **135**, 2589–2592 (1985).
21. Svensson, H. G., Hoogenboom, H. R. & Sjobring, U. Protein LA, a novel hybrid protein with unique single-chain Fv antibody- and Fab-binding properties. *Eur J Biochem* **258**, 890–896 (1998).
22. Eliasson, M. *et al.* Chimeric IgG-binding receptors engineered from staphylococcal protein A and streptococcal protein G. *J Biol Chem* **263**, 4323–4327 (1988).
23. Kihlberg, B. M., Sjobring, U., Kastern, W. & Bjorck, L. Protein LG: a hybrid molecule with unique immunoglobulin binding properties. *J Biol Chem* **267**, 25583–25588 (1992).
24. Yang, H. *et al.* Evolutionary selection of a combinatorial phage library displaying randomly-rearranged various single domains of immunoglobulin (Ig)-binding proteins (IBPs) with four kinds of Ig molecules. *BMC Microbiol* **8**, 137 (2008).
25. Jiang, S. H. *et al.* Alternate arrangement of PpL B3 domain and SpA D domain creates synergistic double-site binding to VH3 and Vkappa regions of fab. *DNA Cell Biol* **27**, 423–431 (2008).
26. Cao, J. *et al.* Novel evolved immunoglobulin (Ig)-binding molecules enhance the detection of IgM against hepatitis C virus. *PLoS one* **6**, e18477 (2011).
27. Qi, P. *et al.* In vitro evolutionary selection of a combinatorial phage library displaying randomly-rearranged various binding domains of SpA and SpG with four human IgG subclasses. *Chinese journal of biotechnology* **28**, 1093–1105 (2012).
28. Inganas, M., Johansson, S. G. & Sjoquist, J. Further characterization of the alternative protein-A interaction of immunoglobulins: demonstration of an Fc-binding fragment of protein A expressing the alternative reactivity. *Scand J Immunol* **14**, 379–388 (1981).
29. Sasso, E. H., Silverman, G. J. & Mannik, M. Human IgM molecules that bind staphylococcal protein A contain VHIII H chains. *J Immunol* **142**, 2778–2783 (1989).
30. Vidal, M. A. & Conde, F. P. Alternative mechanism of protein A-immunoglobulin interaction the VH-associated reactivity of a monoclonal human IgM. *J Immunol* **135**, 1232–1238 (1985).
31. Guss, B. *et al.* Structure of the IgG-binding regions of streptococcal protein G. *EMBO J* **5**, 1567–1575 (1986).
32. Xu Rong, W. P., Yijun, S., Qiuli, C., Xin, P., Chunzhi, F., Zhongtian, Q., Yanjun, L. & Songhua, D. Construction of a novel phagemid pCANTAB5S. *Acta Universitatis Medicinalis* **2004**, 4 (2004).
33. Cao, J. *et al.* Phage-based molecular directed evolution yields multiple tandem human IgA affibodies with intramolecular binding avidity. *J Biotechnol* **158**, 120–127 (2012).
34. Derrick, J. P. & Wigley, D. B. Crystal structure of a streptococcal protein G domain bound to an Fab fragment. *Nature* **359** (1992).

## Acknowledgments

We thank the National Natural Science Foundation of China (No.30872405, 30872246, 30972632, 30972799), the Shanghai Committee of Science and Technology (No.08JC1405200), the Chinese National Key Special Project for the Prevention and Control of Major Infectious Diseases (2009ZX10004-105), the Chinese National Key Special Project for Major New Drug Discovery (2011ZX09506-001), and the National 863 Project (2014AA021403).

## Author contributions

P.P.Q. carried out the construction and selections of the phage displayed library with eight IgG molecules, and the Fig. 1. Y.-Y.D. and X.Y.L. carried out the SPR assay and purification of antibodies, and prepared the Fig. 7. H.T. and T.Y. prepared the Fig. 2. Q.L.C. and J.J.F. prepared and purified proteins. J.H.W., M.M.C., H.P., H.M.Z. and J.C. prepared the Fig. 3. P.P.Q. performed the Fig. 4, 5 and 6. W.P. conceived and designed the original project. W.P. and P.P.Q. wrote the manuscript and analyzed the data. All authors reviewed the manuscript.

## Additional information

**Competing financial interests:** The authors declare no competing financial interests.

**How to cite this article:** Qi, P. *et al.* In vitro molecular evolution yields an NEIBM with a potential novel IgG binding property. *Sci. Rep.* **4**, 6908; DOI:10.1038/srep06908 (2014).



This work is licensed under a Creative Commons Attribution-NonCommercial-NoDerivs 4.0 International License. The images or other third party material in this article are included in the article's Creative Commons license, unless indicated otherwise in the credit line; if the material is not included under the Creative Commons license, users will need to obtain permission from the license holder in order to reproduce the material. To view a copy of this license, visit <http://creativecommons.org/licenses/by-nc-nd/4.0/>